

Nano-inclusion with uniform internal strain induced by a screw dislocation

M. DAI^{1,2}), P. SCHIAVONE²), C.-F. GAO¹)

¹)*State Key Laboratory of Mechanics and Control of Mechanical Structures
Nanjing University of Aeronautics and Astronautics
Nanjing 210016, China
e-mail: cfgao@nuaa.edu.cn*

²)*Department of Mechanical Engineering
University of Alberta
Edmonton, Alberta T6G 1H9, Canada
e-mails: mdai1@ualberta.ca, P.Schiavone@ualberta.ca*

THIS PAPER ADDRESSES THE QUESTION of whether it is possible to design a nano-inclusion (characterized here by the incorporation of interface effects along the material interface) to achieve a screw dislocation-induced uniform internal strain field when a composite is subjected to anti-plane shear deformation. We demonstrate the existence of such an inclusion by identifying its shape via a conformal mapping with unknown coefficients obtained through a system of nonlinear equations. Our numerical examples verify that the inclusion shape is dependent on its size and the specific uniform internal strain field. We show also that the inclusion shape is available even with increasing distance between the inclusion and dislocation. This latter fact leads to the additional conclusion that non-circular nano-inclusions which achieve uniform internal strain fields do indeed exist in a composite subjected to uniform remote anti-plane shear loading.

Key words: dislocation, nano-inclusion, interface effect, size dependence, uniform internal strain field.

Copyright © 2016 by IPPT PAN

1. Introduction

DISLOCATION-INCLUSION INTERACTIONS CONTINUE to receive considerable attention in the literature mainly because of their role in strengthening and hardening mechanisms for heterogeneous materials such as alloys and composites. Initial researches in this area were undertaken using the simplifying assumption that the bond between the inclusion and its surrounding matrix was ‘perfect’ (both traction and displacement are assumed to be continuous across the material interface). For example, DUNDURS and MURA [1] derived the exact elastic field inside a circular inclusion under the influence of an edge dislocation; STAGNI and LIZZIO [2] studied the interaction between an edge dislocation and elliptical

inclusions of various aspect ratios (see also [3, 4]); while GONG and MEGUID [5] considered the effect of a screw dislocation on the elastic field around an elliptical inclusion. In particular, the basic solution for dislocation-inclusion interactions have found wide application in the fracture analysis of fiber-reinforced composites (see, for example, [6, 7]).

Most recently, nano-materials and nano-structures have attracted considerable attention in the literature mainly because of their unique mechanical and physical properties. It is well-known that as the size of an inclusion approaches the nanoscale, separate interfacial effects caused by the contributions of interface energy and interface tension (usually neglected at higher order length scales) become much more significant in the description of deformation of the corresponding composite. As a result, the elastic fields around nano-inclusions are essentially size-dependent [8–11]. More recently, using the Gurtin–Murdoch model [12, 13] of interface elasticity to incorporate interface effects, the size-dependent elastic fields inside circular and elliptical nano-inclusions induced by dislocations, have been investigated by FAN and LIU [14], LUO and XIAO [15] and SHODJA *et al.* [16]. In addition, WANG and SCHIAVONE [17] have proposed a series solution for the interaction problem of a screw dislocation and an arbitrarily-shaped nano-inclusion.

The primary objective of the study of the interaction between dislocations and inclusions is to predict the dislocation-induced interfacial elastic field in an effort to prevent failure of the material interface which inevitably leads to the failure of the composite structure. One possible way to reduce stress concentration in the interface and thus slow interfacial failure is to design special inclusion shapes which induce uniform internal stress fields (thereby eliminating stress peaks, known to be one of the major causes of failure) [18–22]. To the authors’ knowledge, such investigations in the case when a *dislocation* is the major contributor to deformation, remain almost absent from the literature even in the simplest case when the inclusion-matrix interface is assumed to be perfectly bonded. In this paper, we address this matter and examine the existence and construction of such special shapes of inclusion which achieve uniform internal stress in the presence of a dislocation and interface effects. Using the Gurtin–Murdoch model [12, 13], a simple new method is developed to construct a nano-inclusion (i.e. incorporating interfacial effects into the model of deformation) which achieves a prescribed uniform internal strain field induced by a screw dislocation within an infinite elastic solid subjected to anti-plane shear.

A detailed problem description is given in Section 2. In Section 3, using complex variable methods, we identify the desired inclusion shape using conformal mapping techniques. Various numerical examples are given in Section 4 where we also study the size-dependent effect of the dislocation on the shape of the

inclusion and the convergence of the inclusion shape with decaying dislocation-inclusion interaction. We summarize our main results in Section 5.

2. Problem description

In the context of anti-plane shear deformations, we consider a nano-sized elastic inclusion S_1 whose boundary/shape is described by the curve L embedded in an infinite elastic matrix S_0 . The shear modulus of the inclusion is denoted by G_1 while that of the matrix is given by G_0 . Henceforth, superscripts 0 and 1 are used to identify the corresponding quantities in S_0 and S_1 , respectively. As shown in Fig. 1, the inclusion-matrix composite interacts with a screw dislocation with Burgers vector b_z located at the point (x_{10}, x_{20}) . No remote loading is imposed on the matrix. We will determine the shape of the inclusion L which ensures a uniform internal strain field as a result of the dislocation-inclusion interaction.

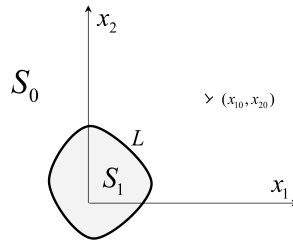


FIG. 1. A nano-inclusion and a screw dislocation in an infinite matrix.

In the theory of anti-plane shear, the out-of-plane displacement w and the anti-plane shear stresses $(\sigma_{13}, \sigma_{23})$ within the matrix and inclusion satisfy, respectively,

$$(2.1) \quad \frac{\partial^2 w^{(i)}}{\partial x_1^2} + \frac{\partial^2 w^{(i)}}{\partial x_2^2} = 0, \quad i = 0, 1;$$

$$(2.2) \quad \sigma_{13}^{(i)} = G_i \frac{\partial w^{(i)}}{\partial x_1}, \quad \sigma_{23}^{(i)} = G_i \frac{\partial w^{(i)}}{\partial x_2}, \quad i = 0, 1.$$

Across the inclusion-matrix interface L , using the Gurtin–Murdoch model of interface elasticity [12, 13], the displacement w and the anti-plane shear traction σ_{n3} satisfy

$$(2.3) \quad w^{(1)} - w^{(0)} = 0, \quad \text{on } L,$$

$$(2.4) \quad \sigma_{n3}^{(1)} - \sigma_{n3}^{(0)} = G_s \frac{d^2 w^{(1)}}{ds^2}, \quad \text{on } L.$$

Here, ds denotes the arc length of an infinitesimal element of the curve L along its tangent, while G_s describes the separate shear modulus describing the interfacial elasticity.

To the authors' knowledge, the problem of the identification of the inclusion shape L which guarantees a uniform internal strain field, induced solely by the presence of a dislocation, remains almost absent from the literature even in the idealized case when interfacial (nano) effects are absent (perfect interface model). In what follows, we introduce a new method to address this deficiency and consider the general case in which interfacial elasticity is included in the model of the inclusion-matrix interface. Our method proceeds by first prescribing the uniform internal strain field within a certain admissible range and subsequently identifying the shape L with the desired property.

3. Solution procedure

3.1. Complex variable methods

The general solutions of Eqs. (2.1) and (2.2) can be represented in the form [19]

$$(3.1) \quad w^{(i)} = \text{Im}[f_i(z)], \quad i = 0, 1,$$

$$(3.2) \quad \sigma_{23}^{(i)} + I\sigma_{13}^{(i)} = G_i F_i'(z), \quad i = 0, 1,$$

where $f_i(z)$ ($z = x_1 + Ix_2$, $i = 0, 1$) denote complex potentials in the matrix and inclusion defined in the regions S_i ($i = 0, 1$), respectively. The letter I is used here to denote the imaginary unit to avoid confusion with the use of the symbol i as a subscript or superscript. Based on the problem description from Section 2, the two complex potentials $f_0(z)$ and $f_1(z)$ take the form of

$$(3.3) \quad f_0(z) = \frac{b_z}{2\pi} \ln(z - z_0) + g_0(z), \quad z_0 = x_{10} + Ix_{20},$$

$$(3.4) \quad f_1(z) = \Gamma_1 z + c_1,$$

where the prescribed uniform internal strain field, given here by $\Gamma_1/2$, can be restricted within a certain admissible range to ensure the existence of solution for the present problem, c_1 is an unknown complex constant to be determined while $g_0(z)$ is holomorphic in the infinite region S_0 . Without loss of generality we stipulate that $\lim_{|z| \rightarrow +\infty} g_0(z) = 0$.

Note that the shear tractions $\sigma_{n3}^{(i)}$ ($i = 0, 1$) on the interface L can be written in terms of $f_i(z)$ ($i = 0, 1$) as [23]

$$(3.5) \quad \sigma_{n3}^{(i)} = -G_i \text{Re} \left[f_i'(t) \frac{dt}{ds} \right], \quad t \in L, \quad i = 0, 1,$$

where dt is an infinitesimal element of the curve L along its tangent and ds is the arc length of dt . By using (3.1) and (3.5), the interface condition (2.3) becomes

$$(3.6) \quad \text{Im}[f_0(t)] = \text{Im}[f_1(t)], \quad t \in L,$$

while the integral of the interface condition (2.4) is simplified as

$$(3.7) \quad \text{Re}[f_0(t)] = \frac{G_1}{G_0} \text{Re}[f_1(t)] + \frac{G_s}{G_0} \text{Im} \left[f_1'(t) \frac{dt}{ds} \right], \quad t \in L.$$

Here, we ignore the constant of integration so that the arbitrary real part of the complex constant c_1 introduced in Eq. (3.4) is now defined uniquely. Substituting Eqs. (3.3) and (3.4) into the conditions (3.6) and (3.7) leads to

$$(3.8) \quad g_0(t) = At + B\bar{t} + \frac{G_s}{G_0} \text{Im} \left[\Gamma_1 \frac{dt}{ds} \right] - \frac{b_z}{2\pi} \ln(t - z_0) + C, \quad t \in L,$$

with

$$(3.9) \quad \begin{aligned} A &= 0.5(1 + G_1/G_0)\Gamma_1, \\ B &= 0.5(G_1/G_0 - 1)\bar{\Gamma}_1, \\ C &= 0.5(G_1/G_0 - 1)\bar{c}_1 + 0.5(1 + G_1/G_0)c_1, \end{aligned}$$

where A and B are known constants determined by the given shear moduli of the inclusion and matrix and the prescribed uniform internal strain field, while C is an unknown complex constant to be determined in the solution process.

In what follows, we will determine the unknown shape L of the inclusion based on the condition for the existence of such a holomorphic function $g_0(z)$ in the infinite region S_0 which satisfies the boundary condition (3.8) with (3.9).

3.2. Existence of the complex potential $g_0(z)$

The simply-connected region S_1 of the inclusion can be defined by the following conformal mapping which maps the exterior of the boundary L (or equivalently the infinite region S_0) in the z -plane to the exterior of the unit circle (denoted by $\sigma = e^{i\theta}$) in the ξ -plane [24],

$$(3.10) \quad z = \omega(\xi) = R \left(\xi + \sum_{j=1}^{+\infty} a_j \xi^{-j} \right), \quad |\xi| \geq 1,$$

where the (known) real constant R characterizes the size of the inclusion and the unknown complex coefficients a_j ($j = 1 \cdots +\infty$) determine the actual shape of the inclusion. In particular, it follows from the definition of the conformal

mapping (3.10) that the derivative of $\omega(\xi)$ is required to have no zeros outside the unit circle in the ξ -plane [24].

By using mapping (3.10), the derivative dt/ds along the boundary L in Eq. (3.8) can be expressed in terms of $\omega(\sigma)$ on the unit circle ($\sigma = e^{I\theta}$) in the ξ -plane as [23]

$$(3.11) \quad \frac{dt}{ds} = \frac{I\sigma\omega'(\sigma)}{|\omega'(\sigma)|},$$

so that the boundary value $g_0(t)$ (see Eq. (3.8)) of the function $g_0(z)$ on the boundary L in the z -plane can be rewritten on the unit circle in the ξ -plane as

$$(3.12) \quad g_0(\omega(\sigma)) = A\omega(\sigma) + B\overline{\omega(\sigma)} + \frac{G_s}{G_0} \operatorname{Re} \left[\Gamma_1 \frac{\sigma\omega'(\sigma)}{|\omega'(\sigma)|} \right] - \frac{b_z}{2\pi} \ln[\omega(\sigma) - z_0] + C.$$

In order to ensure the existence of the function $g_0(z)$ holomorphic in the infinite region S_0 (which is equivalent to ensuring the existence of the function $g_0(\omega(\xi))$ holomorphic outside the unit circle in the ξ -plane), the boundary value $g_0(\omega(\sigma))$ (see (3.12)) of the function $g_0(\omega(\xi))$ on the unit circle in the ξ -plane should satisfy the following necessary and sufficient condition [24],

$$(3.13) \quad \frac{1}{2\pi} \int_0^{2\pi} g_0(\omega(\sigma)) \sigma^{-i} d\theta = 0, \quad \sigma = e^{I\theta}, \quad i = 0, 1, 2, \dots$$

Using Eq. (3.10) and introducing

$$(3.14) \quad b_i = \frac{1}{2\pi} \int_0^{2\pi} \operatorname{Re} \left[\Gamma_1 \frac{\sigma\omega'(\sigma)}{|\omega'(\sigma)|} \right] \sigma^{-i} d\theta, \quad \sigma = e^{I\theta}, \quad i = 0, 1, 2, \dots,$$

$$(3.15) \quad d_i = \frac{1}{4\pi^2} \int_0^{2\pi} \ln[\omega(\sigma) - z_0] \sigma^{-i} d\theta, \quad \sigma = e^{I\theta}, \quad i = 0, 1, 2, \dots,$$

the condition (3.13) results in

$$(3.16) \quad \gamma R b_0 - b_z d_0 + C = 0,$$

$$(3.17) \quad A + B\bar{a}_1 + \gamma b_1 - \frac{b_z}{R} d_1 = 0, \quad B\bar{a}_i + \gamma b_i - \frac{b_z}{R} d_i = 0, \\ \left(\gamma = \frac{G_s}{G_0 R}, \quad i = 2, 3, \dots \right),$$

in which the parameters A , B , γ , R and b_z are all known while the unknown coefficients a_j ($j = 1 \cdots + \infty$) introduced from the mapping (3.10) will determine the actual shape of the inclusion. In particular, Eq. (3.17) shows that the unknown inclusion shape is determined not only by the elastic constants of the bulk and the interface, the dislocation and the prescribed uniform internal strain field but also the size of the inclusion. In what follows, the infinite series from the mapping (3.10) of the region S_1 will be truncated to an N th-order polynomial in N unknown coefficients a_j ($j = 1 \dots N$), to be obtained from the corresponding N nonlinear equations (3.17). Numerical methods will be employed to obtain these N coefficients by solving the N equations (3.17) following which the unknown constant C can be determined from Eq. (3.16). The complex constant c_1 introduced in Eq. (3.4) is then obtained uniquely from the relation (3.9) relating c_1 to C .

3.3. Newton–Raphson iteration

By defining two vectors $\boldsymbol{\alpha}$ and $\mathbf{F}(\boldsymbol{\alpha})$ from the real and imaginary parts of the truncated coefficients a_j ($j = 1, \dots, N$),

$$\begin{aligned}
 \boldsymbol{\alpha} &= \begin{bmatrix} \text{Re}(a_1) \\ \text{Im}(a_1) \\ \vdots \\ \text{Re}(a_N) \\ \text{Im}(a_N) \end{bmatrix}, \\
 \mathbf{F}(\boldsymbol{\alpha}) &= \begin{bmatrix} \text{Re}(A + B\bar{a}_1) \\ \text{Im}(A + B\bar{a}_1) \\ \text{Re}(B\bar{a}_2) \\ \text{Im}(B\bar{a}_2) \\ \vdots \\ \text{Re}(B\bar{a}_N) \\ \text{Im}(B\bar{a}_N) \end{bmatrix} + \gamma \begin{bmatrix} \text{Re}(b_1) \\ \text{Im}(b_1) \\ \vdots \\ \text{Re}(b_N) \\ \text{Im}(b_N) \end{bmatrix} - \frac{b_z}{R} \begin{bmatrix} \text{Re}(d_1) \\ \text{Im}(d_1) \\ \vdots \\ \text{Re}(d_N) \\ \text{Im}(d_N) \end{bmatrix},
 \end{aligned}
 \tag{3.18}$$

the truncated real form of Eq. (3.17) can be rewritten as

$$\mathbf{F}(\boldsymbol{\alpha}) = \mathbf{0},
 \tag{3.19}$$

and the related Jacobian matrix $[\partial\mathbf{F}(\boldsymbol{\alpha})/\partial\boldsymbol{\alpha}]$ can be obtained from the expressions (3.14) and (3.15). The iterative process is then given by

$$\boldsymbol{\alpha}^{(p+1)} = \boldsymbol{\alpha}^{(p)} - \left[\frac{\partial\mathbf{F}(\boldsymbol{\alpha})}{\partial\boldsymbol{\alpha}} \Big|_{\boldsymbol{\alpha}=\boldsymbol{\alpha}^{(p)}} \right]^{-1} \mathbf{F}(\boldsymbol{\alpha}^{(p)}), \quad p = 0, 1, \dots,
 \tag{3.20}$$

where the superscript “ -1 ” indicates the inverse of the Jacobian matrix and $\boldsymbol{\alpha}^{(p)}$ represents the value of the vector $\boldsymbol{\alpha}$ after the p -th iteration.

To guarantee convergence of the iterative process (3.20), the initial value $\boldsymbol{\alpha}^{(0)}$ will be given here by, say, that corresponding to a circle of radius R in the z -plane. If the iterative process (3.20) does not converge for any reasonable initial values $\boldsymbol{\alpha}^{(0)}$, it most likely indicates that the prescribed uniform internal strain field cannot be achieved with the assumed set of elastic constants (bulk and interface), size of the inclusion and location of the dislocation. In addition, even a convergent solution can be considered inadmissible if either the corresponding curve L is self-intersecting in the z -plane or the derivative of the corresponding mapping (3.10) has zeros outside the unit circle in the ξ -plane.

It should be emphasized that although we have not derived a simple necessary and sufficient condition in terms of the prescribed parameters of the problem (elastic constants of the bulk and interface, size of the inclusion, dislocation, and prescribed uniform internal strain field) which guarantees the existence of the required inclusion shape, our numerical results indicate the uniqueness of our solution in that the iterative process consistently converges to the identical inclusion shape for reasonable distinct sets of initial values.

4. Numerical examples

Previous studies have shown that the interfacial shear modulus G_s is of the order of 1 N/m [25, 26] and may take positive or negative values depending on the crystallographic orientation [27, 28], while the shear modulus G_0 of the matrix is of the order of 10 GPa. Consequently, the parameter G_s/G_0 is of the order of 10^{-10} m and we can see from the parameter γ in Eq. (3.17) that incorporation of the interface effect will impact the shape of the inclusion containing a uniform internal strain field only when the inclusion size R decreases toward the nanoscale. In the examples which follow, we adopt the dimensionless parameters γ and z_0/R (see (3.17)) to describe the size-dependent interface effect and the relative location of the dislocation. The convergence of the iterative process (3.20) for a given N is demonstrated by the fact that the relative error between the vectors $\boldsymbol{\alpha}$ of the shape coefficients a_j ($j = 1, \dots, N$) corresponding to two adjacent iterations is less than 10^{-8} , while the final convergence of the inclusion shape is demonstrated by the fact that the relative error between the mapping (3.10) corresponding to two adjacent values of N is less than 0.01%. Our extensive numerical examples (including all examples described below) confirm that a moderately large number N ($20 \leq N \leq 30$) is sufficient to achieve reasonably accurate shape convergence with relative error less than 0.01%.

4.1. The prescribed uniform internal strain field

For the present problem of dislocation-inclusion interaction, since it is well-known that no standard inclusion shapes are able to achieve uniform internal strain fields, we can simply prescribe the uniform internal strain field inside the unknown inclusion based on the average internal strain field induced by a dislocation inside, for example, a circular inclusion. To this end, for a circular inclusion (of radius R incorporating interface effects) interacting with a dislocation at z_0 , the complex potential $f_1(z)$ of the inclusion is given by [14]

$$(4.1) \quad f_1(z) = \sum_{i=1}^{+\infty} m_i z^i + c_1, \quad z \in S_1,$$

with

$$(4.2) \quad m_i = \frac{-b_z}{i\pi z_0^i (1 + G_1/G_0 + i\gamma)}, \quad i = 1, 2, \dots,$$

$$c_1 = \frac{b_z}{2\pi} [G_0 \ln |z_0|/G_1 + I \operatorname{Arg}(-z_0)],$$

where the parameter γ is defined as in Eq. (3.17) and the average strain field inside the circular inclusion can be calculated as

$$(4.3) \quad \Gamma_1^{\text{average}} = \frac{\iint_{S_1} f_1'(z) dx_1 dx_2}{\pi R^2} = m_1$$

$$= \frac{-b_z}{\pi z_0 (1 + G_1/G_0 + \gamma)}.$$

Using Eq. (4.3), the prescribed uniform internal strain field inside our unknown inclusion is defined by introducing a perturbation as follows:

$$(4.4) \quad \Gamma_1 = \frac{-b_z(1 + \eta)}{\pi z_0 (1 + G_1/G_0 + \gamma)},$$

where η is a complex parameter. In particular, for given shear moduli of the inclusion and matrix, it follows from Eq. (3.17) that the actual shape (ignoring the orientation) of the inclusion that achieves a prescribed uniform internal strain field given by Eq. (4.4) is determined by only the parameter γ corresponding to the size-dependent interface effect, the perturbation parameter η and the relative distance $|z_0|/R$ between the dislocation and the inclusion. This result is also verified by our numerical analysis. Consequently, for convenience, in the following numerical examples the dislocation will always occupy a position on the positive x -axis.

4.2. Size-dependent shape of an inclusion with interface effect that achieves uniform internal strain field induced by a dislocation

The size-dependent phenomenon of the elastic field around an inclusion with interface effect is well-known in the literature. Here, our numerical results will show that the shape of an inclusion with interface effect which achieves a uniform internal strain field under the influence of a dislocation is also size-dependent. Figures 2 and 3 illustrate this size-dependence when the inclusion increases in size from the nano-scale to the macro-scale.

Note that the inclusion shapes shown in Figs. 2 and 3 for different inclusion sizes are normalized by their respective inclusion size to facilitate comparisons.

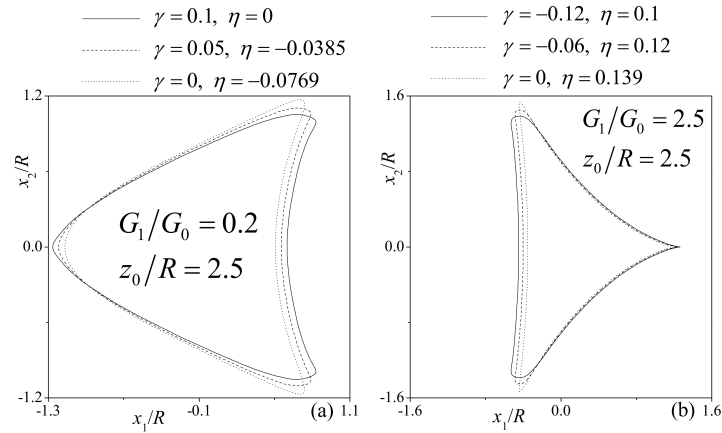


FIG. 2. Effect of dislocation on the shape of an inclusion with interface effect that achieves a uniform internal strain field for real η with increasing size of the inclusion.

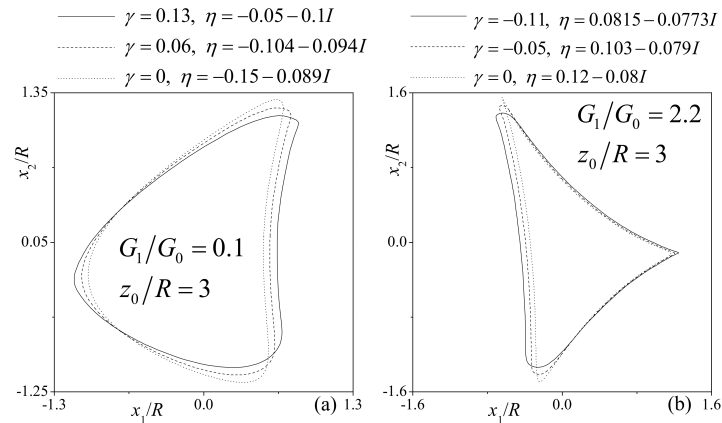


FIG. 3. Effect of dislocation on the shape of an inclusion with interface effect that achieves a uniform internal strain field for complex η with increasing size of the inclusion.

In Figs. 2 and 3 all of the inclusions of different size are able to achieve the same uniform internal strain field under the same relative distance between inclusion and dislocation. It follows that the clear size-dependence of the inclusion shape is caused mainly by the size-dependent interface effect determined by γ . It is interesting to note from Figs. 2 and 3 that soft and hard inclusions seem to be repelled and attracted, respectively, by the dislocation to achieve a uniform internal strain field.

4.3. Convergent effect of dislocation on the inclusion shape that achieves uniform internal strain field with increasing distance between the inclusion and dislocation

It is clear that the distance between the inclusion and the dislocation has a significant impact on the shape of inclusion able to sustain a uniform internal strain field. It is of particular interest, therefore, to examine the effect of the dislocation on the inclusion shape in terms of convergence of the related processes with increasing distance between the inclusion and the dislocation. Shown in Figs. 4 and 5 is the convergence of the nano-inclusion shape with interface effect that achieves a uniform internal strain field when the distance between the inclusion and dislocation increases.

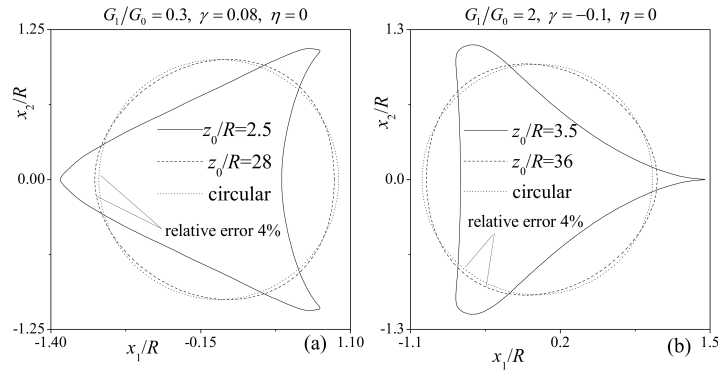


FIG. 4. Convergence of the shape of a nano-inclusion which achieves a uniform internal strain field for $\eta = 0$ with increasing distance between the dislocation and inclusion.

In Fig. 4, we can see that the shape of nano-inclusion which achieves a uniform internal strain field for $\eta = 0$ converges to a circle with increasing distance between the inclusion and dislocation. This is actually not surprising given that the expression (4.1) with (4.2) indicates that the internal strain field inside a circular nano-inclusion induced by a dislocation tends toward a uniform field (given by the average internal strain field (4.3)) with increasing distance between the inclusion and dislocation. The reason why the inclusion shape achieving a uni-

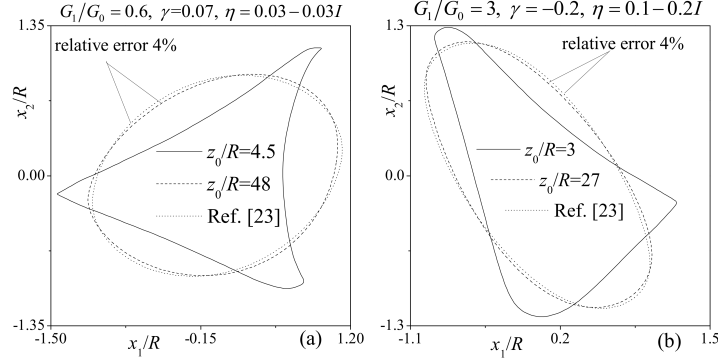


FIG. 5. Convergence of the shape of a nano-inclusion that achieves a uniform internal strain field for complex η with increasing distance between the inclusion and dislocation.

form internal strain field converges when the distance between the inclusion and dislocation increases can perhaps be explained as follows. For a sufficiently large distance between the inclusion and dislocation, the logarithmic term related to the dislocation in the boundary condition (3.8) has the following first-order asymptotic form

$$(4.5) \quad \ln(t - z_0) = \ln(-z_0) - \sum_{j=1}^{+\infty} \frac{t^j}{j z_0^j} \approx \ln(-z_0) - \frac{t}{z_0}, \quad |z_0| \gg |t|.$$

From Eq. (4.5), we see that, with increasing distance between the inclusion and dislocation, the effect of the dislocation on the inclusion shape approximates the equivalent scenario of a uniform remote loading on the inclusion shape. Consequently we can see in Fig. 5 that the shape of a nano-inclusion with uniform internal strain field induced by a screw dislocation is indeed consistent

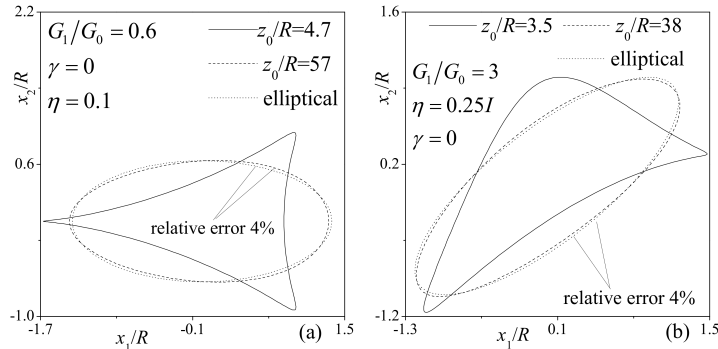


FIG. 6. Convergence of the shape of an inclusion without interface effect which achieves a uniform internal strain field with increasing distance between the dislocation and inclusion.

with that of a nano-inclusion with the same uniform internal strain field under uniform remote anti-plane shear loadings (see [23]) when the distance between the inclusion and dislocation is enough large. Here, an additional example (in which the interface effect is ignored – see Fig. 6) is given to verify this reasoning.

It is seen quite clearly that when the distance between the inclusion and dislocation increases, the non-elliptical inclusion that achieves a uniform internal strain field under the influence of a dislocation, in the absence of any interface effect does indeed converge to the corresponding case of an equivalent elliptical inclusion subjected to the corresponding uniform remote strain field $-b_z/(2\pi z_0)$. Moreover, by comparing Fig. 5 with Fig. 6, it is found that for a given relative error, the presence of interfacial effects will accelerate the convergence of the inclusion shape.

5. Conclusions

A new method is developed to examine the existence and construction of a single inclusion incorporating interfacial elasticity (interface effect) which achieves a uniform internal strain field under the influence of a screw dislocation within an elastic solid subjected to anti-plane shear deformations. The unknown shape of the inclusion is defined by a conformal mapping whose unknown coefficients are determined by a system of nonlinear equations. Numerical examples are given to investigate size-dependency and the convergence of the method towards the desired inclusion shape. In particular, we draw the following important conclusions:

- (1) Whether or not interface effects are included in the model of deformation, we have demonstrated the existence of a single inclusion which achieves a uniform internal strain field induced by a screw dislocation in an infinite elastic solid subjected to anti-plane shear. In particular, the shape of such an inclusion is dependent on the inclusion size (in the case of an inclusion with interface effect) and the specific uniform internal strain field.
- (2) When the distance between the inclusion and dislocation increases, our method continues to converge to the shape of an inclusion (with or without interface effect) which achieves uniform internal strain field. In the case of such an inclusion shape in the absence of interface effects we obtain clear converge to the corresponding elliptical inclusion.
- (3) A consequence of the above conclusion ((2)) is that there do indeed exist non-circular nano-inclusions (with interface effect) that achieve uniform internal strain fields in an elastic solid subjected to uniform remote anti-plane shear.

We conclude by noting that the analogous investigations in plane elasticity present formidable challenges and will form the basis of a subsequent paper.

Acknowledgments

The authors would like to thank an anonymous reviewer whose comments have led to improvements in the manuscript. Dai appreciates the support of the China Scholarship Council. Dai and Gao acknowledge the support of the National Natural Science Foundation of China (11232007&11472130) and a Project Funded by the Priority Academic Program Development of Jiangsu Higher Education Institutions (PAPD). Schiavone thanks the Natural Sciences and Engineering Research Council of Canada for their support through a Discovery Grant (Grant # RGPIN 155112).

References

1. J. DUNDURS, T. MURA, *Interaction between an edge dislocation and a circular inclusion*, J. Mech. Phys. Solids, **12**, 177–189, 1964.
2. L. STAGNI, R. LIZZIO, *Shape effects in the interaction between an edge dislocation and an elliptical inhomogeneity*, Appl. Phys. A, **30**, 217–221, 1983.
3. M.H. SANTARE, L.M. KEER, *Interaction between an edge dislocation and a rigid elliptical inclusion*, ASME J. Appl. Mech., **53**, 382–385, 1986.
4. W.J. YEN, C. HWU, Y.K. LIANG, *Dislocation inside, outside, or on the interface of an anisotropic elliptical inclusion*, ASME J. Appl. Mech., **62**, 306–311, 1995.
5. S.X. GONG, S.A. MEGUID, *A screw dislocation interacting with an elastic elliptical inhomogeneity*, Int. J. Eng. Sci., **32**, 1221–1228, 1994.
6. M. FAN, D.K. YI, Z.M. XIAO, *A Zener–Stroh crack in fiber-reinforced composites with generalized Irwin plastic zone correction*, Int. J. Mech. Sci., **82**, 81–89, 2014.
7. M. FAN, D.K. YI, Z.M. XIAO, *Generalized Irwin plastic zone correction for a Griffith crack near a coated-circular inclusion*, Int. J. Damage Mech., **24**, 663–682, 2015.
8. P. SHARMA, S. GANTI, *Size-dependent Eshelby’s tensor for embedded nano-inclusions incorporating surface/interface energies*, ASME J. Appl. Mech., **71**, 663–671, 2004.
9. L. TIAN, R. RAJAPAKSE, *Elastic field of an isotropic matrix with a nanoscale elliptical inhomogeneity*, Int. J. Solids Struct., **44**, 7988–8005, 2007.
10. J. LUO, X. WANG, *On the anti-plane shear of an elliptic nano inhomogeneity*, Eur. J. Mech. A Solids, **28**, 926–934, 2009.
11. M. DAI, P. SCHIAVONE, C.F. GAO, *Uniform strain fields inside periodic inclusions incorporating interface effects in anti-plane shear*, Acta Mech., 2016. doi: 10.1007/s00707-016-1660-z.
12. M.E. GURTIN, A.I. MURDOCH, *A continuum theory of elastic material surfaces*, Arch. Ration. Mech. Anal., **57**, 291–323, 1975.

13. M.E. GURTIN, J. WEISSMÜLLER, F. LARCHE, *A general theory of curved deformable interfaces in solids at equilibrium*, Philos. Mag. A, **78**, 1093–1109, 1998.
14. Q.H. FANG, Y.W. LIU, *Size-dependent elastic interaction of a screw dislocation with a circular nano-inhomogeneity incorporating interface stress*, Scripta Mater., **55**, 99–102, 2006.
15. J. LUO, Z.M. XIAO, *Analysis of a screw dislocation interacting with an elliptical nano inhomogeneity*, Int. J. Eng. Sci., **47**, 883–893, 2009.
16. H.M. SHODJA, H. AHMADZADEH-BAKHSAYESH, M.Y. GUTKIN, *Size-dependent interaction of an edge dislocation with an elliptical nano-inhomogeneity incorporating interface effects*, Int. J. Solids Struct., **49**, 759–770, 2012.
17. X. WANG, P. SCHIAVONE, *Interaction of a screw dislocation with a nano-sized, arbitrarily shaped inhomogeneity with interface stresses under anti-plane deformations*, Proc. R. Soc. A, **470**, 20140313, 2014.
18. T.C.T. TING, P. SCHIAVONE, *Uniform antiplane shear stress inside an anisotropic elastic inclusion of arbitrary shape with perfect or imperfect interface bonding*, Int. J. Eng. Sci., **48**, 67–77, 2010.
19. X. WANG, *Uniform fields inside two non-elliptical inclusions*, Math. Mech. Solids, **17**, 736–761, 2012.
20. M. DAI, C.F. GAO, C.Q. RU, *Uniform stress fields inside multiple inclusions in an elastic infinite plane under plane deformation*, Proc. R. Soc. A, **471**, 20140933, 2015.
21. M. DAI, P. SCHIAVONE, C.F. GAO, *Uniform strain field inside a non-circular inhomogeneity with homogeneously imperfect interface in anisotropic anti-plane shear*, Z. Angew. Math. Phys., **67**, 43, 2016.
22. M. DAI, P. SCHIAVONE, C.F. GAO, *Periodic inclusions with uniform internal hydrostatic stress in an infinite elastic plane*, Z. Angew. Math. Mech., 2016; doi: 10.1002/zamm.201500298.
23. M. DAI, C.F. GAO, *Non-circular nano-inclusions with interface effects that achieve uniform internal strain fields in an elastic plane under anti-plane shear*, Arch. Appl. Mech., 2015; doi: 10.1007/s00419-015-1098-0.
24. N.I. MUSKHELISHVILI, *Some Basic Problems of the Mathematical Theory of Elasticity*, Springer Science & Business Media, 2013.
25. J.A. RUUD, A. WITVROUW, F. SPAEPEN, *Bulk and interface stresses in silver-nickel multilayered thin films*, J. Appl. Phys., **74**, 2517–2523, 1993.
26. D. JOSELL, J.E. BONEVICH, I. SHAO, R.C. CAMMARATA, *Measuring the interface stress: Silver/nickel interfaces*, J. Mater. Res., **14**, 4358–4365, 1999.
27. R.E. MILLER, V.B. SHENOY, *Size-dependent elastic properties of nanosized structural elements*, Nanotechnology, **11**, 139–147, 2000.
28. V.B. SHENOY, *Atomistic calculations of elastic properties of metallic fcc crystal surfaces*, Phys. Rev. B, **71**, 094104, 2005.

Received March 23, 2016; revised version May 18, 2016.